Available online at www.eccomasproceedia.org
Eccomas Proceedia SMART (2023) 214-225

ECCOMAS Proceedia

X ECCOMAS Thematic Conference on Smart Structures and Materials
SMART 2023
D.A. Saravanos, A. Benjeddou, N. Chrysochoidis and T. Theodosiou (Eds)

IN-VACUO STRUCTURED FABRIC TUNEABLE VIBRATION ABSORBER

SOFIA BALDINI*, PAOLO GARDONIO*, EMILIANO RUSTIGHI†, C. MALACARNE§, M. PERINI§

* University of Udine – DPIA, Via delle Scienze 206, 33100 Udine, Italy
e-mail: baldini.sofia@spes.uniud.it , paolo.gardonio@uniud.it

† University of Trento – DIE, Via Sommarive 9, 38123 Trento, Italy
e-mail: emiliano.rustighi@unitn.it

§ ProM Facility – Trentino Sviluppo S.p.A., Via Fortunato Zeni 8, 38068 Rovereto (TN), Italy
e-mail: matteo.perini@trentinosviluppo.it

Abstract. This paper is focussed on a new tuneable vibration absorber, which is formed by one or multiple strips of a structured fabrics wrapped in a vacuum bag. The middle span of this beam-like structure is fixed to a post such that its flexural vibration is controlled by a flapping fundamental natural mode, whose natural frequency is varied by changing the level of vacuum in the bag. At first, the study presents a parametric analysis to show how the bending stiffness and damping properties of the beam-like structure vary with respect to the vacuum level in the bag and with respect to the grain geometry and number of fabric layers. Then, it provides a thorough analysis of the absorber base mechanical impedance frequency response function with respect to the level of vacuum and the type of structured fabric. The preliminary experimental results show that the fundamental natural frequency of the proposed tuneable vibration absorber can be varied over a wide frequency range such that it can be effectively used to track changes in the tonal excitations or changes in the resonant response of the hosting structure.

Key words: tuneable vibration absorber, structured fabric, in-vacuo material, adaptive material.

1 INTRODUCTION

The past three decades have seen a growing interest on Tunable Vibration Absorbers (TVA) [1], which can be effectively adopted to control either the harmonic response of mechanical systems subject to time-varying tonal excitations or the resonant response of time-varying mechanical systems subject to broadband stationary stochastic disturbances. Normally, TVA systems rely on electro-mechanical transducers to create a tuneable spring-mass-damper system, such as for example shape memory alloys [2,3], electrorheological and magnetorheological elastomers [4,5], coil-magnet devices connected to electrical shunts [6-10] and piezoelectric patch/stack materials connected to electrical shunts [11-18]. The stiffness of these systems can be controlled electrically such that the fundamental resonance frequency of

Peer-review under responsibility of the organizing committee of SMART 2023.
doi: 10.7712/150123.9779.444503

the absorber can be suitably varied to track either the frequency of the tonal excitation acting on the hosting system or to track the resonance frequency that characterises the resonant response of a time varying hosting system subject to a broadband stochastic excitation. The damping effect of these systems can be varied electrically too, such that the vibration energy absorption for the tonal and broadband excitations can be suitably maximised. Normally, to control tonal vibrations the damping should be set to rather low values, whereas to control broadband resonant vibrations it should be tuned to a critical value [1,19,20].

This paper proposes a novel TVA, which is composed by one or more strips of a structured fabric wrapped in a vacuum bag whose middle span is clamped to the post of the absorber [21]. The flexural vibration of the two-arms beam is thus characterised by a flapping fundamental mode, whose dynamics resembles that of a classical mass-spring-damper vibration absorber. The fabric is made by an interwoven construction of truss-like particles, which has been fabricated using additive manufacturing technology. The material is wrapped in a sealed plastic bag whose interior vacuum pressure is controlled by a miniature pump. The bending stiffness and mechanical loss properties of the beam can then be corrected by varying the vacuum pressure in the bag. Hence, the fundamental resonance frequency and the damping factor of the in-vacuo structured fabric vibration absorber can be tuned online in such a way as to track the frequency of a tonal excitation or to trail changes in the resonant response of the hosting system.

Structured fabrics are composed by a periodic elementary structure that repeats itself in space in such a way as to form a compliant mesh. These structures exhibit quite a loose bending stiffness at ambient pressure. However, recently, Wang *et al.* [22] have proposed a new layout composed by 3-dimensional truss-like particles arranged into multi-layer chain mails, which are wrapped in a vacuum bag. The bending stiffness of this assembly can be suitably varied by changing the level of vacuum in the bag. The research study presented in [22] aimed at providing lightweight, tuneable and adaptive fabrics, for applications in wearable exoskeletons, haptic architectures and reconfigurable medical supports. Hence, their analysis was limited to the static mechanical properties. This study considers instead the dynamic response of such structures with respect to a practical application, that is the tuneable vibration absorber.

The study is structured in two main parts. The first part provides a short description of the structured in-vacuo fabrics and presents the vibration tests carried out to characterise the dynamic bending stiffness and hysteresis properties of the material. The second part presents the frequency measurements of base impedance taken to characterised the dynamic response of the absorber and to investigate the tuning range of its characteristic resonance frequency.

2 IN VACUO STRUCTURED FABRICS DESIGN AND CHARACTERISATION

2.1 Structured fabrics design and fabrication

In general, structured fabrics are composed by a network of rigid elements linked together in such a way as to form an interwoven material. A classic example of this material is given by armour chain mails worn in the middle age by knights and soldiers. In this study, the structured fabric is made of truss-like rigid grains and is wrapped in a sealed plastic bag. As happens for food packaging, e.g. rice or coffee bags, if the pressure in the bag is progressively reduced, then the material becomes more and more stiff. This is due to jamming, that is friction effects,

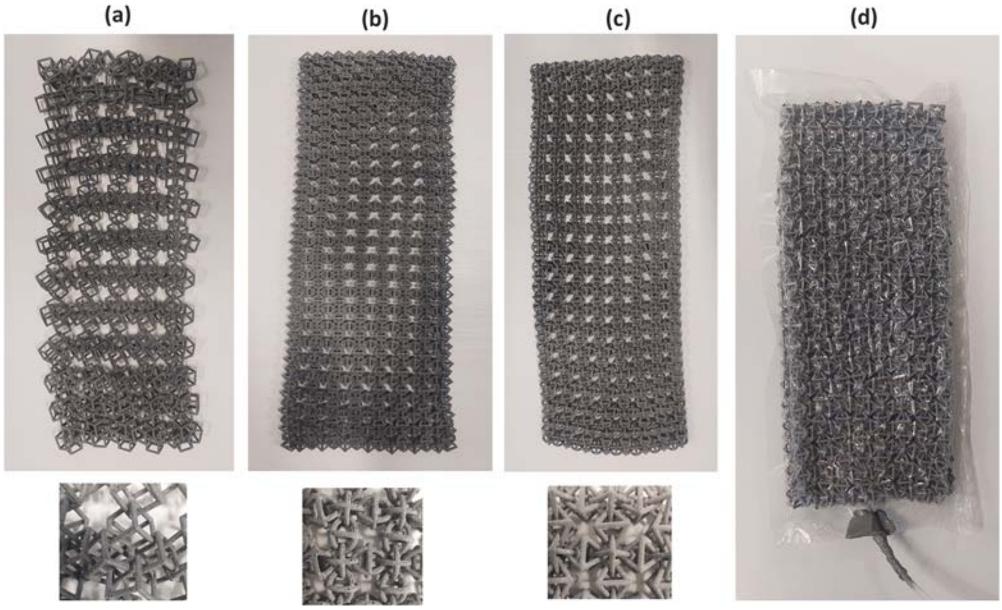

Figure 1: Structured fabrics studied in this paper. (a) spheres, (b) cubes, (c) octahedral. (d) Fabric in a sealed vacuum bag used for the bending stiffness and hysteresis tests.

between the elements of the interwoven structure. The jamming transition, that is the transition from a fluid to a solid state of granular materials [23,24], is a phase transition that depends both on normal (compression only) and shear stress. The material considered in this study is characterised by an interwoven mail, where the rigid elements are looked to each other via both convex and non-convex contacts. The latter are characterised by larger bonding areas and thus generate stronger jamming effects such that the material can sustain rather large normal and shear stresses and does not fall apart when there is no vacuum in the bag [22].

The prototype TVA designed and built for this study, uses structured fabrics made in Nylon PA12 material by 3D printing technology. The fabrics were designed either with a single or double strips such that they resembled a thin and wide beam structure. The plastic skin was home-made starting from off the shelf bags for food packaging. Also, a 3D printed inlet port was built in plastic using 3D printing technology and sealed to the middle span of the plastic bag. In this way the in vacuo structured fabric acted as a two-arms beam clamped in the middle span to the post. The inlet port was designed in such a way as it served both as a connector for the vacuum tube and as a mechanical joint to fix the two-arms in-vacuo structured fabric beam to the hosting mechanical system. The vacuum was generated with an off the shelf pump and a simple circuit encompassing two valves and a vacuum gauge. Table 1 provides the geometries and principal dimension of the three truss-like particles considered in this study, which are shown in Figure 1. Also, Table 2 gives the physical properties of the Nylon PA12 material used to fabricate the chain mail fabrics. The structured fabrics built for this study have been manufactured by an HP Multi Jet Fusion (MJF) printer. MJF-printed parts can be use both for prototypes and end-used components. With this technology, additive manufacturing does not need support structures and complex post processing operations. During printing, all empty spaces are filled with wasted powder, making MJF prints self-supporting. That same powder is then continuously recycled for the following prints. MJF can be a successful solution for complex designs: it allows parts consolidation and very complex and interconnected geometries, which is generally a problem using alternative technologies such as fused deposition modelling (FDM) or stereolithography (SLA). The result of this manufacturing is shown in Figure 1, where the dimension of the elementary truss grains is of the order of 1 cm^2.

Table 1: Prototyped structured fabrics studied in this paper with dimensions and weight

Name	Geometry	Width (mm)	Length (mm)	Thickness (mm)	Mass (g)
Spheres		100	210	10	49
Octahedra		110	240	15	62
Cubes	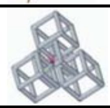	110	190	15	39

Table 2: Nylon PA12 technical specifications

Property	Value
Powder melting point	187°C
Particle Size	60 µm
Density of parts	1.01 g/cm^3
Tensile strength	48 MPa
Tensile modulus	1800 MPa
Elongation at break	15-20%
Bending strength	65-70 MPa
Bending modulus	1730 MPa

2.2 Dynamic stiffness

The dynamic bending stiffness of the two-arms in-vacuo structured fabric beam was first measured with the 6-points bending setup depicted in Figure 2b. This test facility resembles the classical 3-points setups used for static analyses. Here, to perform the dynamic test such that the beam undergoes full cycle positive-negative bending displacements, the setup encompasses twin pinning points for a total of 6-points. Hence, as depicted in Figure 1a, the beam specimen is simply supported in proximity of the two ends and undergoes an imposed transverse displacement w in the middle span. The test rig built for this study was characterised by the following dimensions $a = 80$ mm and l=160 mm. According to theory of solid mechanics, the bending stiffness given by the ratio between the force F and displacement w imposed by the shaker is given by

$$\frac{F}{w} = 48\frac{EI}{l^3} \tag{1}$$

where E is the Young's modulus of elasticity of the material, l is the span between the fixed pinning points and $I = bh^3/12$ is the cross section area moment of inertia, where b and h are the width and thickness of the beam. An equivalent Young's modulus can thus be retrieved for the in-vacuo structured fabric beam, which is given by

$$E = \frac{l^3}{4bh^3}\frac{F_0}{w_0} \tag{2}$$

where F_0/w_0 is the static bending stiffness, which can be retrieved from the dynamic stiffness measurements as the asymptotic value for the circular frequency that tends to 0, i.e. for $\omega \to 0$.

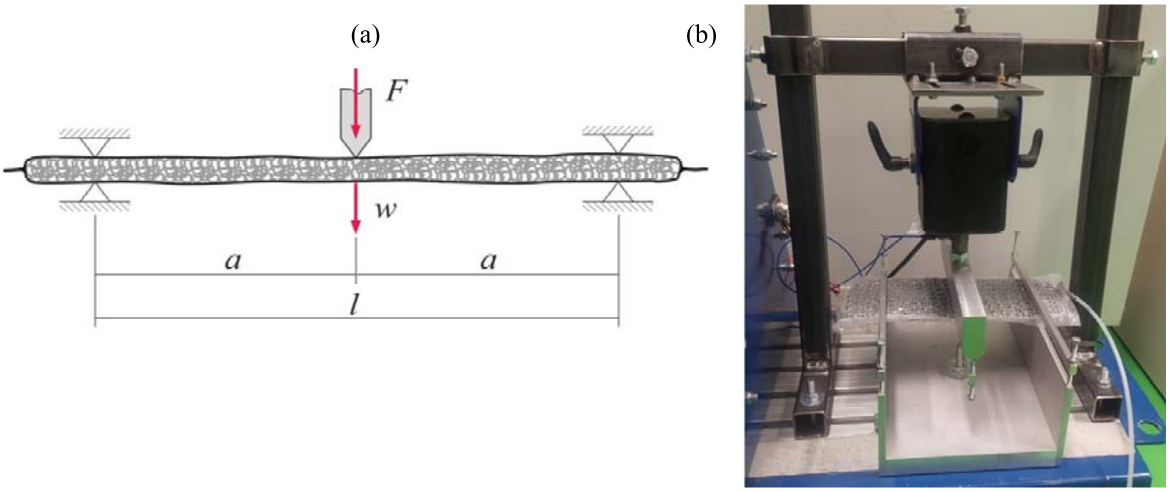

Figure 2: Dynamic material characterization by six-points bending test. (a) schematic showing the excitation points, (b) setup showing the test.

As shown in Figure 1d and Figure 2b, the in-vacuo structured fabric beams were prepared using a heat-sealed plastic bag encompassing a small plastic tube connected to the vacuum equipment, which was composed by a vacuum pump, a vacuum-meter, and a sealing valve. The dynamic stiffness FRFs were measured in a frequency range comprised between 5 and 40 Hz. Two set of tests were carried out encompassing either a single or a double layer of each structured fabric. The tests were run with the following levels of confining vacuum pressures: 80 kPa, 60 kPa, 40 kPa, 20 kPa, 10 kPa and 5 kPa.

Figures 3 to 5 show the modulus and phase of the dynamic bending stiffness FRFs, $K(\omega) = F(\omega)/w(\omega)$, measured on the in-vacuo beams encompassing either a single (left hand side plots) or a double (right hand side plots) layer of sphere, cube, octahedral fabrics. Each plot shows six spectra obtained for the six confining vacuum pressures. All plots show the typical spectrum of the bending dynamic stiffness measured at the middle-span of a pinned-pinned beam. The modulus and phase spectra show a low frequency stiffness-type response with constant amplitude and phase 0°, followed by a reversed peak due the resonance of the beam fundamental bending mode. At higher frequencies the modulus and phase spectra show a mass-type response characterised by a 40 dB/decade rising amplitude and phase $+180°$.

As summarised in Figure 6 and Table 3, the bending stiffness of the in-vacuo structured fabrics increases as the vacuum level in the bags is raised. Consequently, the resonance frequency too tends to raise as the level of vacuum in the bags is increased. The double layer configurations offer comparatively higher bending stiffnesses, and thus larger resonance frequencies, than the single layer configurations. For the single layer configuration, the cubic fabric presents the highest bending stiffness; in contrast, for a double layer configuration, the octahedral fabric offers the most rigid structure. The fabric made with cubes is characterised by the largest range of stiffnesses, and thus of resonance frequencies. With the two-layers cubic fabric configuration, the stiffness can be doubled in the given range of vacuum pressure. Also, the results for octahedral structured fabric show that the stiffness can be incremented by about 5 times with the addition of one more layer of structured fabric. The results of this experimental study show that the fabrics are characterised by neighbouring but separate ranges of stiffness such that a rather large range of stiffnesses could be generated with beams encompassing multiple layers made from different types of grains. According to Table 3, if higher ranges of stiffness were required, it would be better to use cubic double layer structures. Instead for lower stiffness ranges, it would be preferable to use spherical or octahedral structured fabrics.

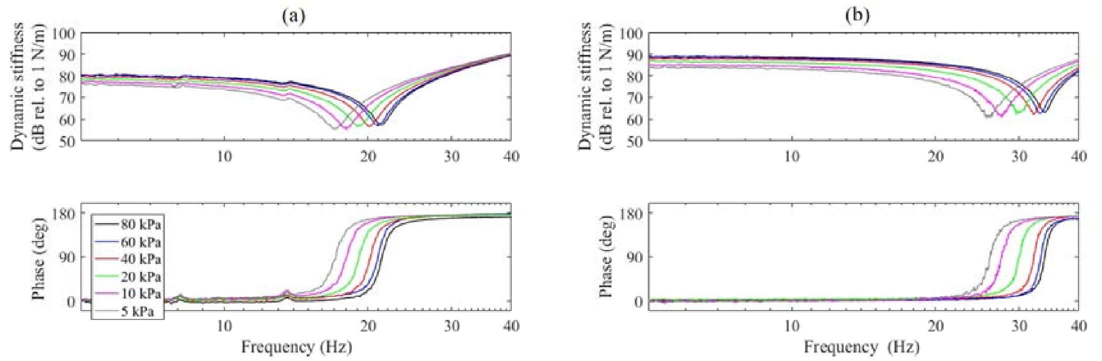

Figure 3: Dynamic stiffness for cube-grains structured fabrics. (a) single layer (b) double layer.

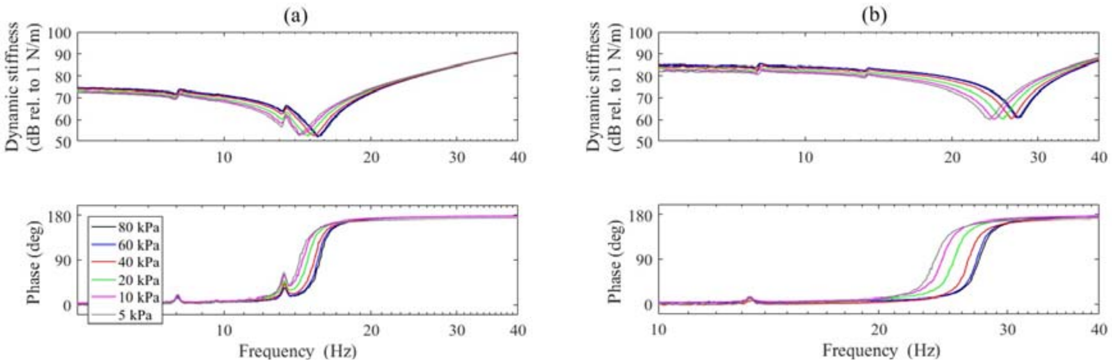

Figure 4: Dynamic stiffness for sphere-grains structured fabrics. (a) single layer (b) double layer.

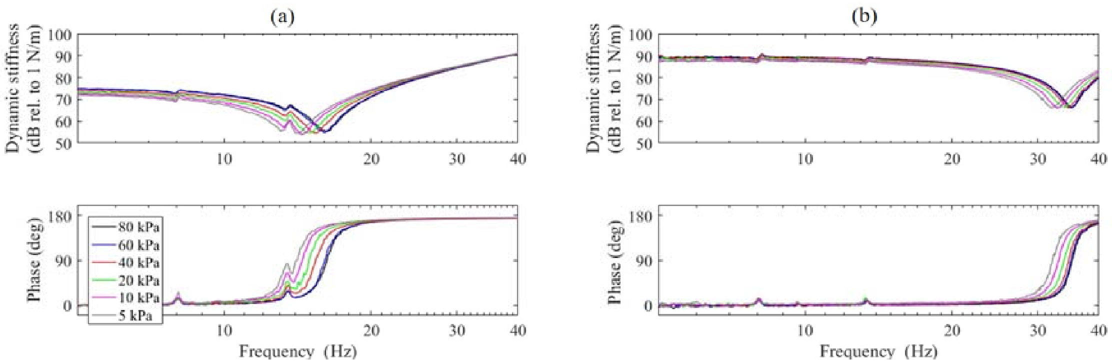

Figure 5: Dynamic stiffness for octaedra-grains structured fabrics. (a) single layer (b) double layer.

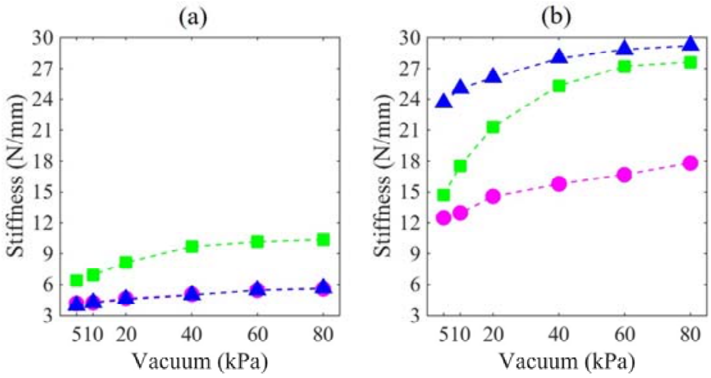

Figure 6: Stiffness of the tuneable structured fabrics assembled with one (a) or two (b) overlapped layers. The points represent the measured data. Sphere-grains (magenta), octahedra grains (blue) cube-grains (green).

Table 3: Range of stiffness variability depending of geometry and overlapped layers

Geometry	One layer stiffness range (N/mm)	Two layers stiffness range (N/mm)
Cubes	≈ 5,5 – 10	≈ 14 – 28
Spheres	≈ 4 – 5,5	≈ 12,5 – 18
Octahedra	≈ 4 – 5,5	≈ 24 – 30

2.3 Hysteresis loops at resonance frequency

The FRFs depicted in Figures 3 to 5 show rounded resonance peaks, which indicate the in-vacuo structured fabric beams are characterised by significant levels of damping. To better investigate this feature, displacement-velocity, i.e. phase, diagrams were recorded for time-harmonic excitations, which confirmed the presence of hysteresis elliptic loops, that is linear material damping. Therefore, according to the literature [25], a Voight damping model given by a damper in parallel with a spring was employed. As a result, the material loss factor value was calculated with respect to the total energy dissipated in a harmonic cycle ΔE_c, which is given by the area of the hysteresis loop, and with respect to the peak strain potential energy U_m, which is given by the product of the peak elastic force and peak displacement, such that [26]:

$$\eta = \frac{\Delta E_c}{2\pi U_m} \tag{3}$$

Figure 8 shows the loss factors derived from measured hysteresis loops for the three types of single- and double-layer fabrics with respect to different level of vacuum pressure. The graphs confirm indeed a non-trivial loss factor effect, which interestingly maintains quite a constant value comprised between 5% and 7% with respect to the type of grain, the number of layers and the vacuum pressure. This is quite an interesting feature for the TVA application, particularly because it suggests the stiffness, and thus the fundamental resonance frequency of the material, can be suitably tuned without affecting the damping level. This seems to suggest that, for the vacuum level considered in these measurements the grains are heavily jammed to each other. There is thus little friction effect to generate large material damping effects.

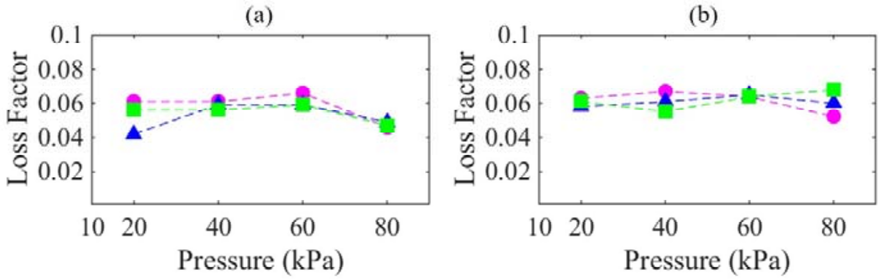

Figure 8: Structural loss factor of the tuneable structured fabrics assembled with one (a) or two (b) overlapped layers. The points represent the measured data. Magenta for spheres, blue for octahedra and green for cubes.

3 TUNABLE VIBRATION ABSORBER DESIGN AND CHARACTERISATION

3.1 TVA design and fabrication

As anticipated in the Introduction, the in-vacuo structured fabric beam can be used as a tuneable vibration absorber device. To this end, as shown in Figure 9, a specially dedicated post has been fixed at the middle span of the in-vacuo structured fabric beam The post has been designed and built with 3D printing technology in such a way as it performs two tasks. First, it provides the mechanical base junction of the TVA with the hosting structure or mechanical system to be controlled. Second, is provides a plug-in junction for the air suction pipe. A small diameter flexible tube was thus fixed on one side to the TVA joint and on the other side to the vacuum setup, which was composed by a pump, a vacuo-meter and a check valve.

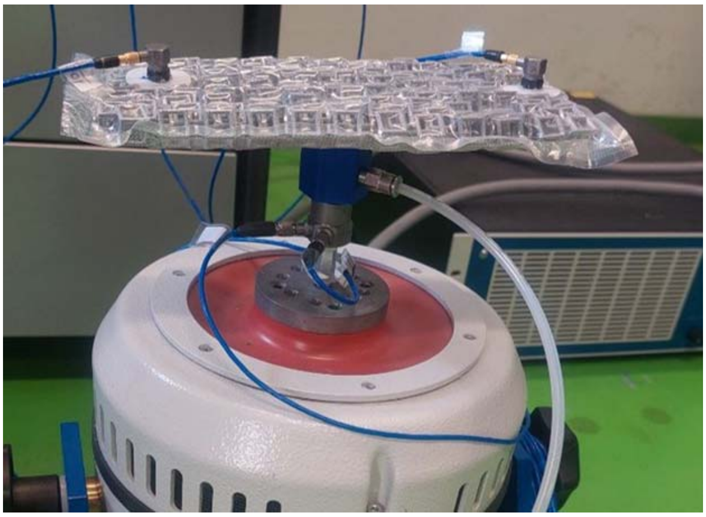

Figure 9: TVA test set up.

3.2 Base impedance FRF

To characterise the vibration absorption properties of the TVA system, base impedance FRF measurements were taken with the setup shown in Figure 9. The measurement system is composed by a large shaker whose vibrating platform was instrumented with an impedance head. The base joint of the TVA was promptly screwed into the load cell. The two terminations of the in-vacuo structured fabric beam were equipped with two accelerometers to measure and reconstruct the flapping natural mode that should characterise the flexural response of the in-vacuo structured fabric beam.

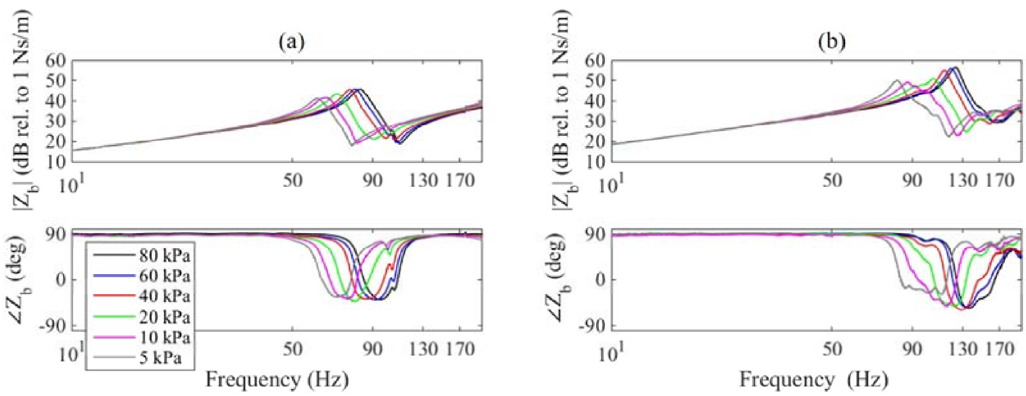

Figure 10: Impedance response for cubes assembled with one (a) or two (b) overlapped layers.

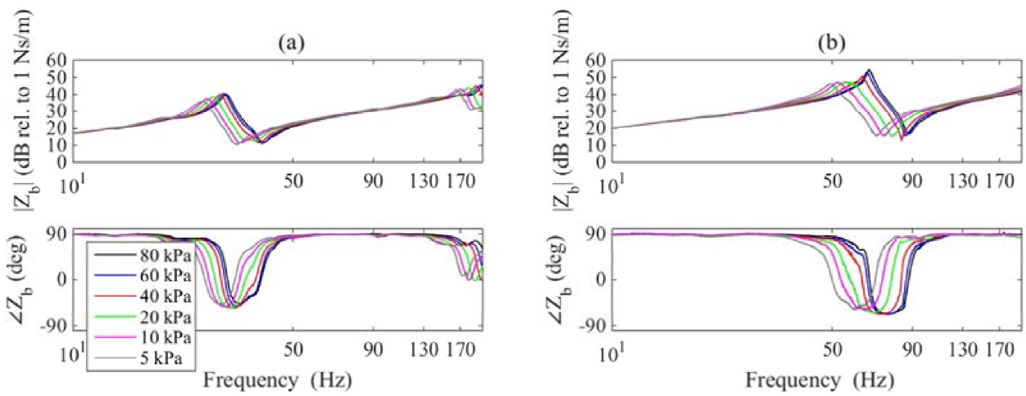

Figure 11: Impedance response for spheres assembled with one (a) or two (b) overlapped layers.

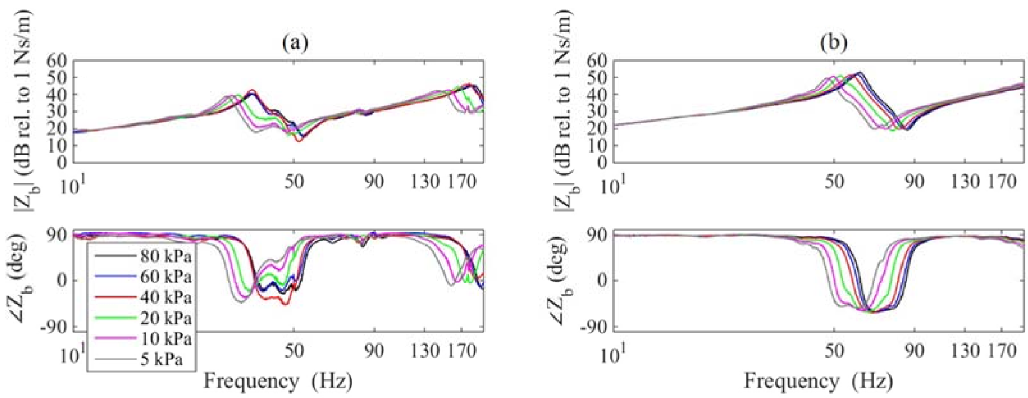

Figure 12: Impedance response for octahedra assembled with one (a) or two (b) overlapped layers.

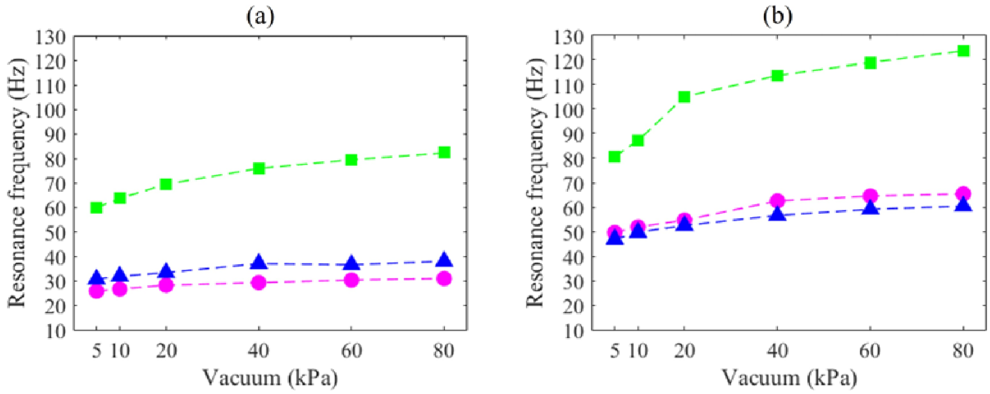

Figure 13: Measured resonance frequency of the tuneable structured fabrics assembled with one (a) or two (b) overlapped layers. Magenta for spheres, blue for octahedra and green for cubes.

Figures 10 to 12 show the modulus and phase of the base impedance FRFs, $Z(\omega) = F(\omega)/\dot{w}(\omega)$, measured on the in-vacuo beams encompassing either a single (left hand side plots) or a double (right hand side plots) layer of sphere, cube, octahedral structured fabrics. As for the dynamic stiffness analyses, each plot shows six spectra obtained for the six confining vacuum pressures reported above. The spectra show the typical base impedance of a seismic mass connected to a base mass via a spring damper lumped element. Indeed, as discussed in Ref. [27] for example, at low frequencies the spectrum is characterised by a modulus that rises proportionally to the circular frequency and a constant phase value of about $+90°$. There is then a resonance peak followed by an antiresonance through, with the phase that initially falls down to $-90°$ and then recovers to $+90°$. At higher frequencies the spectrum shows again a modulus that rises proportionally to the circular frequency and a phase that maintains the $+90°$ value. All this indicates that at low and high frequencies the device presents a mass effect. More precisely, the measurements taken with the accelerometers have shown that at low frequencies the in-vacuo structured fabric beam behaves as a solid body together with the junction component, with negligible flapping effects. Therefore, the base impedance is given by the whole mass of the beam and base component. Alternatively, at higher frequencies, despite the base vibrations, the two ends of the in-vacuo structured fabric are characterised by little vibrations such that the base impedance is controlled by the mass of the base component. At resonance frequency the two ends of the in-vacuo structured fabric display large counter oscillations to the base oscillations, which generate the desired vibration absorption effect. The extent of these oscillations is controlled by the damping of the in-vacuo structured beam. Normally, to counteract harmonic vibrations, the TVA is tuned in such a way as it resonates at the tonal disturbance and its damping is kept to the minimum possible value such that the hosting structure faces a large impedance load. Alternatively, for broadband vibrations the TVA is tuned in such a way it resonates at the resonance frequency of the hosting system, but in this case the damping is brought up such that the double resonant response of the combined hosting structure-TVA modes is optimally dampened.

Overall, the plots shown in Figures 10 to 12 together with those reported in Figure 13 indicate that the resonance frequency of the TVAs can be suitably shifted to higher/lower values by increasing/lowering the level of vacuum in the bags. For the 5 to 80 kPa pressure range, the single layer TVAs are characterised by resonance frequencies comprised between 60-85 Hz (cube grains), 25-30 Hz (sphere grains), 30-40 Hz (octahedra grins). Alternatively, the double layer TVAs are characterised by resonance frequencies comprised between 80-125 Hz (cube grains), 50-65 Hz (sphere grains), 45-60 Hz (octahedra grains). This confirms that the resonance frequency of the TVAs can be suitably tuned over significant ranges by varying the vacuum pressure. Moreover, these ranges can be further enlarged by adopting multiple layers with combinations of different grains.

4 CONCLUSIONS

This paper has investigated the vibration response of a new tuneable vibration absorber, which is made by a structured fabric strip wrapped in a vacuum bag, which has been fixed in the middle span to a post. The paper has shown that the bending stiffness of the in vacuo structured fabric beam can be suitably varied by changing the vacuum pressure in the bag. This effect depends on the type of elementary truss grains of the fabric and on the number of layers wrapped in the bag. For instance, the cubic and octahedral fabrics offers the highest bending stiffness respectively for the single- and double-layer configurations. When the vacuum pressure is raised from 5 to 80 kPa, the stiffness of two-layers cubic fabric beam is doubled. Also, the double layer octahedral structured fabric shows 5 times higher stiffness than the single layer one. These properties can be suitably employed to shift the resonance frequency of the fundamental flapping flexural mode of the structured fabric beam, that is, of the tuneable vibration absorber. In this respect, the study has shown that, for 5 to 80 kPa pressure range, the resonance frequency of either the single- or double-layer vibration absorbers can be increased by 30% to 40%. Also, the resonance frequency of the double layer vibration absorbers is about 50% higher than that of the single layer absorber. This suggests that rather wide tuning ranges can be achieved with designs encompassing multiple layers and different types of elementary truss grains. The study has also showed that the beam is characterised by small losses, with a structural loss factor that does not change significantly with the level of vacuum in the bag as well as with respect to the number of layers and the type of elementary grains. In general, the loss factor is comprised between 5% and 7%. This is a rather important feature, which indicates that the vibration absorber resonance frequency can be tuned independently from the absorber damping effect.

REFERENCES

[1] J. P. Den Hartog, *Mechanical Vibrations*, Fourth ed. New York: McGraw-Hill, 1986.

[2] K. Williams, G. Chiu, and R. Bernhard, "Adaptive-Passive Absorbers Using Shape-Memory Alloys," *Journal of Sound Vibration*, vol. 249, pp. 835–848, Jan. 2002.

[3] E. Rustighi, M. J. Brennan, and B. R. Mace, "A shape memory alloy adaptive tuned vibration absorber: design and implementation," *Smart Materials and Structures*, vol. 14, no. 1, pp. 19–28. 2004.

[4] S. B. Kumbhar, S. P. Chavan, and S. S. Gawade, "Adaptive tuned vibration absorber based on magnetorheological elastomer-shape memory alloy composite," *Mechanical Systems and Signal Processing*, vol. 100, pp. 208–223, Feb. 2018.

[5] E. Rustighi, D. F. Ledezma-Ramirez, P. E. Tapia-Gonzalez, N. Ferguson, and A. Zakaria,

"Modelling and experimental characterisation of a compressional adaptive magnetorheological elastomer isolator," *Journal of Vibration and Control*, vol. 28, no. 21–22, pp. 3093–3107, Jun. 2021.
[6] D. Niederberger, S. Behrens, A. J. Fleming, S. O. R. Moheimani, and M. Morari, "Adaptive electromagnetic shunt damping," *IEEE/ASME Transactions on Mechatronics*, vol. 11, no. 1. 2006.
[7] C. Paulitsch, P. Gardonio, and SJ. Elliott, "Active vibration damping using an inertial electrodynamic actuator," *J Vib Acoust*, vol. 129, pp. 39–47, 2007.
[8] T. Inoue, Y. Ishida, and M. Sumi, "Vibration Suppression Using Electromagnetic Resonant Shunt Damper," *Journal of Vibration and Acoustics*, vol. 130, no. 4, Jul. 2008.
[9] E. Turco and P. Gardonio, "Sweeping shunted electro-magnetic tuneable vibration absorber: Design and implementation," *Journal of Sound and Vibration*, vol. 407, pp. 82–105, Oct. 2017.
[10] P. Gardonio, E. Turco, A. Kras, L. D. Bo, and D. Casagrande, "Semi-active vibration control unit tuned to maximise electric power dissipation," *Journal of Sound and Vibration*, vol. 499. 2021.
[11] S. Wu, "Piezoelectric shunts with a parallel R-L circuit for structural damping and vibration control," *SPIE Proceedings*, pp. 259–269, May 1996.
[12] N. W. Hagood and A. von Flotow, "Damping of structural vibrations with piezoelectric materials and passive electrical networks," *Journal of Sound and Vibration*, vol. 146, no. 2, pp. 243–268. 1991.
[13] O. Thomas, J. Ducarne, and J.-F. Deü, "Performance of piezoelectric shunts for vibration reduction," *Smart Materials and Structures*, vol. 21, no. 1, p. 015008, 2011.
[14] N. Alujević, I. Tomac, and P. Gardonio, "Tuneable vibration absorber using acceleration and displacement feedback," *Journal of Sound and Vibration*, vol. 331, no. 12, pp. 2713–2728, Jun. 2012.
[15] P. Gardonio and D. Casagrande, "Shunted piezoelectric patch vibration absorber on two-dimensional thin structures: Tuning considerations," *Journal of Sound and Vibration*, vol. 395, 2017.
[16] P. Gardonio, M. Zientek, and L. Dal Bo, "Panel with self-tuning shunted piezoelectric patches for broadband flexural vibration control," *Mechanical Systems and Signal Processing*, vol. 134, 2019.
[17] J. Høgsberg, "Vibration control by piezoelectric proof-mass absorber with resistive-inductive shunt," *Mechanics of Advanced Materials and Structures*, vol. 28, no. 2, pp. 141–153, Jan. 2019.
[18] G. Konda Rodrigues, P. Gardonio, L. Dal Bo, and E. Turco, "Piezoelectric patch vibration control unit connected to a self-tuning RL-shunt set to maximise electric power absorption," *Journal of Sound and Vibration*, vol. 536, p. 117154, Oct. 2022.
[19] M.J. Brennan, N.S. Ferguson, Vibration, in: F. Fahy, J. Walker (Eds.), Advanced Applications in Acoustics, Noise and Vibration, pp. 530–580, CRC Press, London, 2004.
[20] M. Zilletti, S. J. Elliott, and E. Rustighi, "Optimisation of dynamic vibration absorbers to minimise kinetic energy and maximise internal power dissipation," *Journal of Sound and Vibration*, vol. 331, no. 18, pp. 4093–4100, Aug. 2012.
[21] E. Rustighi, P. Gardonio, N. Cignolini, S. Baldini, C. Malacarne, and M. Perini, "Vibration response of tuneable structured fabrics," presented at the International Conference on Noise and Vibration Engineering (ISMA 2022), Katholieke Universiteit Leuven, Belgium.
[22] Y. Wang, L. Li, D. Hofmann, J. E. Andrade, and C. Daraio, "Structured fabrics with tunable mechanical properties," *Nature*, vol. 596, no. 7871, pp. 238–243, Aug. 2021.
[23] R. P. Behringer and B. Chakraborty, "The physics of jamming for granular materials: a review," *Reports on Progress in Physics*, vol. 82, no. 1, p. 012601, 2018.
[24] A. J. Liu and S. R. Nagel, *Jamming and rheology: constrained dynamics on microscopic and macroscopic scales*. London: Taylor & Francis, 2001.
[25] D. I. G. Jones, *Handbook of viscoelastic vibration damping*. New York: J. Wiley, 2001.
[26] A. D. Nashif, D. I. G. Jones, and J. P. Henderson, *Vibration damping*. John Wiley & Sons, 1991.
[27] J. Rohlfing, P. Gardonio, and S. J. Elliott, "Base impedance of velocity feedback control units with proof-mass electrodynamic actuators," *Journal of Sound and Vibration*, vol. 330, 2011.